Matters Arising

Cell

Control of the Assembly of ATP- and ADP-Actin by Formins and Profilin

David R. Kovar,[1,5] Elizabeth S. Harris,[4] Rachel Mahaffy,[1] Henry N. Higgs,[4] and Thomas D. Pollard[1,2,3,*]
[1] Department of Molecular, Cellular, and Developmental Biology
[2] Department of Cell Biology
[3] Department of Molecular Biophysics and Biochemistry
Yale University, New Haven, CT 06520, USA
[4] Department of Biochemistry, Dartmouth Medical School, Hanover, NH 03755, USA
[5] Present address: Departments of Molecular Genetics and Cell Biology and of Biochemistry and Molecular Biology, The University of Chicago, Chicago, IL 60637, USA.
*Contact: thomas.pollard@yale.edu
DOI 10.1016/j.cell.2005.11.038

SUMMARY

Formin proteins nucleate actin filaments, remaining processively associated with the fast-growing barbed ends. Although formins possess common features, the diversity of functions and biochemical activities raised the possibility that formins differ in fundamental ways. Further, a recent study suggested that profilin and ATP hydrolysis are both required for processive elongation mediated by the formin mDia1. We used total internal reflection fluorescence microscopy to observe directly individual actin filament polymerization in the presence of two mammalian formins (mDia1 and mDia2) and two yeast formins (Bni1p and Cdc12p). We show that these diverse formins have the same basic properties: movement is processive in the absence or presence of profilin; profilin accelerates elongation; and actin ATP hydrolysis is not required for processivity. These results suggest that diverse formins are mechanistically similar, but the rates of particular assembly steps vary.

INTRODUCTION

The list of formin-dependent actin-based cellular structures is growing rapidly and includes cytokinetic cleavage furrows, yeast actin cables, adherens junctions, and filopodia (Chang et al., 1997; Evangelista et al., 2002; Feierbach and Chang, 2001; Kobielak et al., 2004; Pellegrin and Mellor, 2005; Sagot et al., 2002a; Schirenbeck et al., 2005; Severson et al., 2002). The formin family is large and diverse with three fission yeast formin genes, each involved in a distinct cellular function (Chang et al., 1997; Feierbach and Chang, 2001; Petersen et al., 1998), at least 15 formin genes in mammals and six formin genes in *Drosophila* (Higgs and Peterson, 2005).

The defining feature of formins is the homodimeric formin homology 2 (FH2) domain, which interacts with the barbed end of actin filaments (Pruyne et al., 2002). FH2 domains promote actin filament nucleation (Pruyne et al., 2002; Sagot et al., 2002b) and remain associated with the barbed end as filaments elongate (Higashida et al., 2004; Kovar and Pollard, 2004; Moseley et al., 2004; Romero et al., 2004; Zigmond et al., 2003). FH2 domains generally slow elongation as they "walk" along a growing barbed end, but the effect varies among formins studied to date. Fission yeast Cdc12p completely blocks elongation, budding yeast Bni1p and FRL1 slow elongation, and mammalian mDia1 has no effect on elongation (Harris et al., 2004; Kovar et al., 2003; Kovar and Pollard, 2004; Moseley et al., 2004; Zigmond et al., 2003). FH2 domains and capping proteins interfere with each other's binding to barbed ends (Zigmond et al., 2003; Moseley et al., 2004; Romero et al., 2004). Since both FH2 domains and capping proteins dissociate slowly from barbed ends, the first protein to bind determines the behavior of that filament for an extended time (Kovar et al., 2005). Thus, filaments nucleated by formins can elongate processively for extended periods even in the presence of capping protein (Harris et al., 2004; Kovar et al., 2005; Moseley et al., 2004; Zigmond et al., 2003).

Adjacent to the FH2 domains, FH1 domains are characterized by short runs of consecutive proline residues that bind the actin monomer binding protein profilin (Chang et al., 1997). The number of potential profilin binding sites varies widely, from one to sixteen. Profilin binding to FH1-FH2 domain constructs increases barbed-end elongation rate in association with Cdc12p, Bni1p, and mDia1 (Kovar et al., 2003; Kovar and Pollard, 2004; Romero et al., 2004).

While formins possess common features, the diversity of functions and reported biochemical activities raised the

possibility that formins differ in fundamental ways. For example, Cdc12p is a barbed-end capping protein in the absence of profilin, whereas other formins are not. One study suggested that profilin binding to FH1 is required for processive FH2 movement of mDia1 (Romero et al., 2004), while another showed that profilin is not required for processivity of Bni1p (Kovar and Pollard, 2004). In addition, ATP hydrolysis by newly added actin subunits is proposed to be required for mDia1 processivity (Romero et al., 2004), a property not yet demonstrated for other formins. Some apparent differences may arise from the assays employed to study formins. Actin polymerization is a combination of nucleation and elongation events, which are difficult to differentiate in ''bulk'' samples. This problem is particularly acute for formins, which affect both nucleation and elongation rates.

We employed total internal reflection fluorescence (TIRF) microscopy to observe directly actin polymerization in the presence of four formins: Cdc12p, Bni1p, mDia1, and mDia2. We learned that these diverse formins have the same basic properties: movement is processive in the absence and presence of profilin; elongation is accelerated by profilin; and actin ATP hydrolysis is not required for processivity. We conclude that the four formins studied here employ the same general mechanism for actin filament nucleation and elongation, but that the rates of the reactions vary between them.

RESULTS

For most experiments, we mixed actin monomers with formins and/or profilin in polymerizing buffer and flowed samples into glass microscope cells coated with NEM-myosin II. NEM-myosin II binds filaments randomly along their lengths, maintaining them in the evanescent field while leaving both barbed and pointed ends free to elongate. Actin subunits labeled on cys-374 with Oregon green (OG-actin) allow filament visualization, but unlabeled actin accounts for most of the growth (Amann and Pollard, 2001; Kuhn and Pollard, 2005). Images were acquired every 15 s for up to 30 min. Under these conditions in the absence of other proteins, all filaments grow from the pool of 1.0 μM polymerizable Mg-ATP-actin at rates of 10–11 subunits/s at their barbed ends and 0.30 subunits/s at their pointed ends (Figures 1A–1C). Figure S1 in the Supplemental Data available with this article online illustrates how we analyzed and displayed time-lapse TIRF microscopy data.

Formin-Mediated Assembly of ATP-Actin

When supplied with Mg-ATP-actin monomers, fission yeast Cdc12(FH1FH2)p, budding yeast Bni1(FH1FH2)p, mouse mDia1(FH1FH2), and mouse mDia2(FH1FH2) all nucleate filaments that grow at their barbed ends at a rate characteristic of each formin. All of these filaments grow at their pointed ends the same rate as controls. A few filaments in these samples nucleate spontaneously and grow independently of formin, providing convenient internal controls.

Two distinct populations of filaments assemble in the presence of mouse formin mDia2(FH1FH2) (Figures 1D–1F, S1, and S4). One population consists of control filaments that grow at their barbed ends at rates similar to filaments in the absence of formin (Filament 1). Filaments in the second population grow at their barbed ends at only 1.5 subunits/s (Filament 2), presumably due to modification of the elongation reaction by continuous association of mDia2(FH1FH2) near the elongating barbed end. Three observations support this interpretation: (1) the fraction of filaments with slower-growing barbed ends depends upon the concentration of mDia2(FH1FH2) (Figure S1D); (2) slowly growing filaments occasionally switch to growing at the control rate, which we interpret as mDia2(FH1FH2) dissociation events (Figure S1, Filament 3); and (3) faster-growing filaments occasionally switch to the slower rate, interpreted as mDia2(FH1FH2) binding events (Figure 1F, bottom green curve). If mDia2(FH1FH2) rapidly exchanged on and off barbed ends, all filaments would grow at an intermediate rate.

In contrast, mDia1(FH1FH2) (Figures 1G–1I and S4) or mDia1(FH2) (Figures 1J–1L), which lacks the profilin binding FH1 domain, nucleate filaments that elongate at their barbed ends at the same rate (~10 subunits/s) as control filaments without formin. The single population of filaments makes it impossible for this assay to identify which filaments have mDia1(FH1FH2) associated with their growing barbed ends.

For direct comparison, we include records of filaments growing in the presence of Cdc12(FH1FH2)p (Figures S2A–S2C; Table 1) and Bni1(FH1FH2)p (Figures S2D–S2F). Cdc12(FH1FH2)p completely caps barbed ends (Figure S2B, Filament 2), whereas Bni1(FH1FH2)p slows barbed-end elongation by ~35% (Figure S1E, Filament 2) compared to internal control filaments (Filament 1 in each case; Kovar et al., 2003; Kovar and Pollard, 2004).

Formin-Mediated Assembly of Profilin-ATP-Actin

A low concentration of profilin (2.5 μM) slows barbed-end growth by Mg-ATP-actin (Figures 2A–2C) to 9.1 subunits/s and pointed-end growth to 0.04 subunits/s. In the presence of all four formin FH1FH2 constructs, profilin strongly influences elongation of barbed ends by Mg-ATP-actin monomers (Figures 2 and S3; Table 1).

With mDia1(FH1FH2) and 2.5 μM profilin, two distinct populations of filaments appear (Figures 2G–2I). One population is indistinguishable from control filaments (Filament 1) in both fluorescence intensity and growth rate. Filaments in the second population (Filament 2) are less than half as bright and grow at their barbed ends 4.5 times faster (43.9 subunits/s) than control filaments. The simplest explanation for two populations is that the bright filaments have free barbed ends, whereas the fast-growing dim filaments have mDia1(FH1FH2) bound persistently to their barbed ends. In agreement, (1) the fraction of fast-growing dim filaments depends on the concentration of mDia1(FH1FH2) (data not shown), (2) fast-growing dim filaments occasionally switch to slowly growing a bright segment (Filament 3), apparent mDia1(FH1FH2) dissociation events, and (3) slowly assembling bright filaments occasionally switch to rapid growth of a dim segment (Filament 4), apparent mDia1(FH1FH2) binding events. We believe that formin-associated filaments are

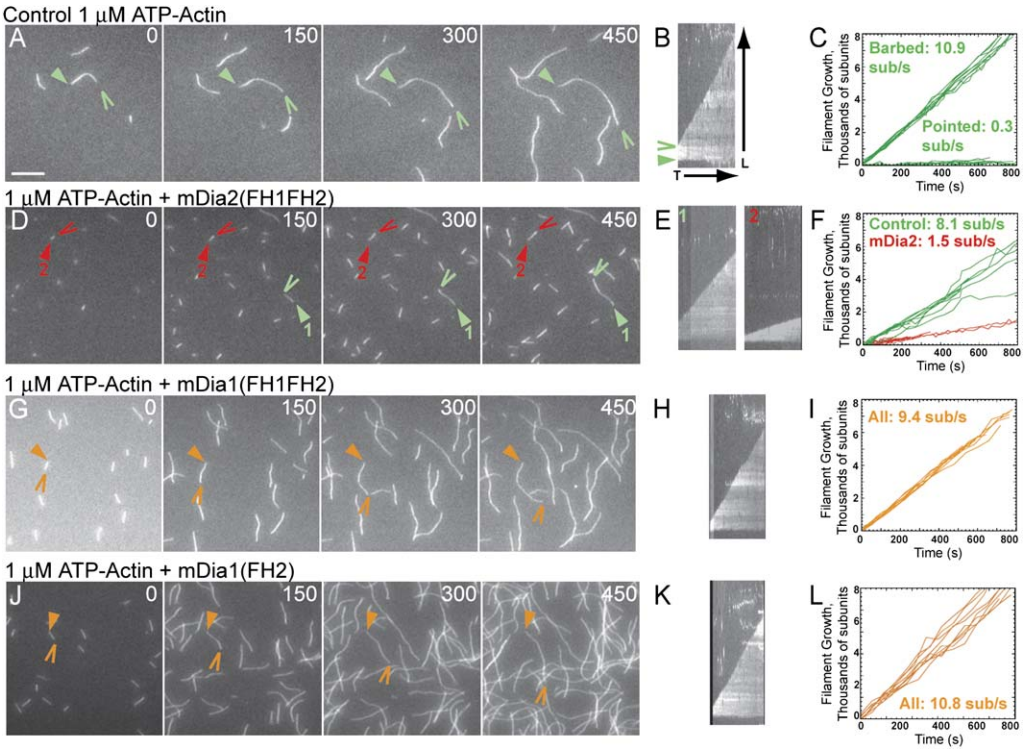

Figure 1. Time-Lapse Evanescent Wave Fluorescence Microscopy of the Effect of Formins on ATP-Actin Polymerization

The spontaneous assembly of 1.0 μM ATP-actin with 0.5 μM ATP-actin labeled with Oregon green (ATP-OG-actin) on slides coated with NEM-myosin II. Conditions: 10 mM imidazole (pH 7.0), 50 mM KCl, 1 mM $MgCl_2$, 1 mM EGTA, 50 mM DTT, 0.2 mM ATP, 50 μM $CaCl_2$, 15 mM glucose, 20 μg/ml catalase, 100 μg/ml glucose oxidase, 0.5% (4000 cP) methylcellulose at 25ºC. Scale bar = 5 μm.

(A, D, G, and J) Time-lapse micrographs with time in seconds indicated at top. Wedges and triangles indicate barbed and pointed ends. Green, red and orange marks indicate control, formin-nucleated, and indistinguishable filaments. Movies of all time lapses are published as Supplemental Data.

(B, E, H, and K) Kymographs of the length (y axis) of the filaments marked to the left versus time (x axis, 900 s).

(C, F, I, and L) Plots of the growth of eight individual filament barbed ends (and pointed ends for [C]) versus time for control and formin-nucleated filaments.

(A–C) 1.0 μM ATP-actin only control.

(D–F) 1.0 μM ATP-actin with 1.0 nM mDia2(FH1FH2). Filament 1: control. Filament 2: mDia2(FH1FH2)-nucleated.

(G–I) 1.0 μM ATP-actin with 1.0 nM mDia1(FH1FH2).

(J–L) 1.0 μM ATP-actin with 1.0 nM mDia1(FH2).

dimmer in the presence of profilin because profilin-actin is the predominant species adding to the end of the filament and that profilin has a lower affinity for OG-actin than unlabeled actin. Actin was labeled with Oregon green on cys-374, which lies within the profilin-actin interaction surface (Schutt et al., 1993). Profilin has a 10-fold weaker affinity for actin labeled on cys-374 with the smaller dye pryene (Vinson et al., 1998).

The combination of profilin with the other three formin FH1FH2 constructs produces effects similar to mDia1 (FH1FH2), but with different rates. Dim formin-dependent filaments elongate faster than bright internal control filaments: Cdc12p is 1.4-fold faster than control filaments; mDia2 is 1.5-fold faster (Figures 2D–2F); and Bni1p is 2.0-fold faster (Table 1). In all cases, dim filaments occasionally become bright (Filament 3) simultaneous with growing at the slower rate, apparent FH1FH2 dissociation events. Conversely, bright filaments occasionally become dim coincident with switching to growth at the faster rate, apparent FH1FH2 binding events. A plot of the fraction of filaments bound to formin versus time shows that each formin allows the addition of tens of thousands of subunits, on average, before dissociating (Figure 3C). The specific off-rates vary between formins by two orders of magnitude: $1.2 \times 10^{-3}\ s^{-1}$ for mDia1(FH1FH2), $1.3 \times 10^{-4}\ s^{-1}$ for mDia2(FH1FH2), $1.3 \times 10^{-4}\ s^{-1}$ for Bni1(FH1FH2)p, and $6.0 \times 10^{-5} s^{-1}$ for Cdc12(FH1FH2)p.

The FH1 domain is required for profilin to enhance formin-mediated barbed-end elongation. The combination of profilin with mDia1(FH2) produces two populations of filaments that differ in both barbed end elongation rate and filament intensity (Figures 2J–2L). Control filament barbed ends grow at 8.7 subunits/s (Filament 1), whereas mDia1(FH2)-dependent filaments are 20% brighter and elongate at only 3.2 subunits/s (Filament 2). Apparently, profilin-ATP-actin adds to FH2-associated filaments, but at only a third the rate of a free barbed end. We believe that FH2-associated filaments are brighter in the presence of profilin because actin/OG-actin is the predominant species adding to the end of the filament and that profilin has a higher affinity for unlabeled actin than OG-actin.

Table 1. Comparison of ATP-Actin Assembly Rates in the Presence of Formin

Conditions[b]	Elongation Rate (Control Filaments[a])	
	Barbed-End Subunits/s	Pointed-End Subunits/s
Spontaneous Assembly[c]		
1 μM actin only	10.9 ± 0.06	0.30 ± 0.04
1 μM actin + 5 μM profilin	9.1 ± 0.1	0.04 ± 0.06
Cdc12(FH1FH2)p	NA[d] (9.6 ± 0.1)	0.31 ± 0.08 (0.1 ± 0.06)
Cdc12(FH1FH2)p + 5 μM profilin	13.3 ± 0.6 (9.6 ± 0.2)	−0.08 ± 0.11 (0.04 ± 0.05)
mDia2(FH1FH2)	1.5 ± 0.1 (8.1 ± 0.2)	0.24 ± 0.08 (0.2 ± 0.1)
mDia2(FH1FH2) + 3.0 μM profilin	12.1 ± 0.7 (8.1 ± 0.1)	0.03 ± 0.04 (−0.2 ± 0.1)
mDia2(FH1FH2) + 3.0 μM profilin-R88E	2.4 ± 0.1 (8.9 ± 0.2)	0.2 ± 0.06 (0.3 ± 0.1)
mDia2(FH1FH2) + 3.0 μM profilin-Y6D	0.5 ± 0.03 (7.1 ± 0.1)	0.05 ± 0.03 (0.04 ± 0.06)
Bni1(FH1FH2)p	5.3 ± 0.5 (8.5 ± 0.1)	0.17 ± 0.12 (0.25 ± 0.04)
Bni1(FH1FH2)p + 1 μM profilin	20.4 ± 1.5 (10.1 ± 0.8)	0.1 ± 0.4 (0.07 ± 0.1)
mDia1(FH1FH2)[e]	9.4 ± 0.2	0.21 ± 0.07
mDia1(FH1FH2) + 3 μM profilin	46.9 ± 0.5 (11.6 ± 0.7)	0.02 ± 0.05 (−0.05 ± 0.04)
mDia1(FH1FH2) + 3 μM profilin-R88E	9.2 ± 0.2	0.4 ± 0.1
mDia1(FH1FH2) + 3 μM profilin-Y6D	3.2 ± 0.1 (8.2 ± 0.1)	−0.04 ± 0.05 (0.05 ± 0.1)
mDia1(FH1[11P]FH2)[f]	8.3 ± 0.1	0.27 ± 0.08
mDia1(FH1[11P]FH2) + 5 μM profilin	48.5 ± 0.7 (8.9 ± 0.5)	−0.03 ± 0.1 (0.03 ± 0.05)
mDia1(FH2)	10.8 ± 0.2	0.3 ± 0.05
mDia1(FH2) + 3 μM profilin	3.2 ± 0.1 (8.7 ± 0.1)	−0.2 ± 0.15 (−0.05 ± 0.05)
Formin Immobilized on Slide[g]		
mDia2(FH1FH2)	1.7 ± 0.04 (7.3 ± 0.05)	NA[h] (0.2 ± 0.07)
mDia2(FH1FH2) + 2.5 μM profilin	7.8 ± 0.4 (8.7 ± 0.6)	NA (0.03 ± 0.04)
Bni1(FH2)p	4.7 ± 0.2 (8.1 ± 0.1)	NA (0.2 ± 0.1)
mDia1(FH1FH2)	5.2 ± 0.1 (6.0 ± 0.2)	NA (0.1 ± 0.05)
mDia1(FH1FH2) + 2.5 μM profilin	11.8 ± 0.2 (4.1 ± 0.1)	NA (−0.2 ± 0.1)
mDia1(FH1[11P]FH2)	3.8 ± 0.04 (4.8 ± 0.07)	NA (0.2 ± 0.05)
mDia1(FH1[11P]FH2) + 2.5 μM profilin	15.3 ± 0.3 (4.9 ± 0.2)	NA (0.01 ± 0.06)

[a] The rates of internal control filaments are reported in parentheses.
[b] At least ten individual filaments were measured for each population. Rates are represented as mean ± SD.
[c] Experiments where formin was not attached to the slide surface, as reported in Figures 1, 2, 3A, and S1–S4. One micromolar unlabeled ATP-actin.
[d] Cdc12-nucleated filaments elongate from their pointed ends only.
[e] The FH1 domain contains five putative profilin-binding proline-rich regions.
[f] The FH1 domain contains 11 putative profilin-binding proline-rich regions.
[g] Experiments where formin was immobilized on the slide, as reported in Figure 4. One micromolar unlabeled ATP-actin with mDia2(FH1FH2) and Bni1(FH2) and 0.5 μM unlabeled ATP-actin with mDia1(FH1FH2) and mDia1(FH1[11P]FH2).
[h] The pointed-end rate is included in the barbed-end rate for filaments elongating from immobilized formin.

Dependence of Formin-Mediated Assembly of ATP-Actin on the Concentrations of Actin and Profilin

Formin-mediated elongation of actin filament barbed ends depends on the concentrations of both actin and profilin (Figure 3). The elongation rate of Mg-ATP-actin alone or in the presence of formin (Figure 3A, open symbols) is directly proportional to the monomer concentration. The slope of the plot with Bni1(FH1FH2)p (Figure 3A, open squares) is about half that of actin alone or actin with mDia1(FH1FH2) (Figure 3A, open diamonds). The presence of 2.5 μM profilin increases the slope of plots of elongation rate versus actin

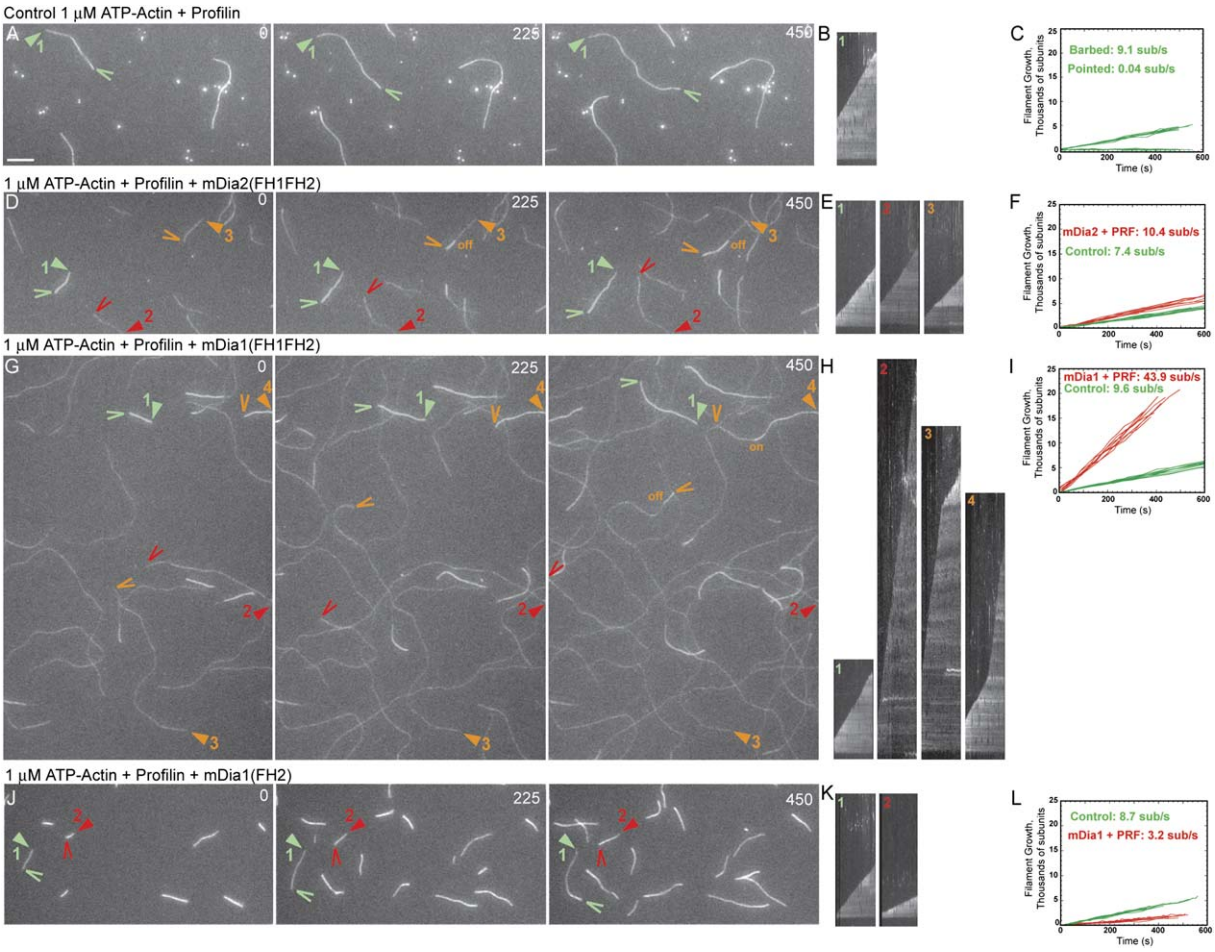

Figure 2. Time-Lapse Evanescent Wave Fluorescence Microscopy of the Effect of Formins on Profilin-ATP-Actin Polymerization

The spontaneous assembly of 1.0 μM ATP-actin with 0.5 μM ATP-OG-actin in the presence of profilin and formin on slides coated with NEM-myosin II. Conditions and symbols as in Figure 1. Scale bar = 5 μm.

(A, D, G, and J) Time-lapse micrographs with time in seconds indicated at top. Green, red, and orange marks indicate control, formin-associated and filaments where formin binds (on) or dissociates (off) during the time course.

(B, E, H, and K) Kymographs of the length (y axis) of the filaments marked to the left versus time (x axis, 900 s).

(C, F, I, and L) Plots of the growth of eight individual filament barbed ends (and pointed ends for [C]) versus time for control and formin-associated filaments.

(A–C) 1.0 μM ATP-actin with 5 μM human profilin (HPRF) control.

(D–F) 1.0 μM ATP-actin with 1 μM HPRF and 1.0 nM mDia2(FH1FH2). Filament 1: control. Filament 2: mDia2(FH1FH2)-associated. Filament 3: mDia2(FH1FH2) dissociates.

(G–I) 1.0 μM ATP-actin with 2.5 μM HPRF and 1.0 nM mDia1(FH1FH2). Filament 1: control. Filament 2: mDia1(FH1FH2)-associated. Filament 3: mDia1(FH1FH2) dissociates. Filament 4: mDia1(FH1FH2) binds.

(J–L) 1.0 μM ATP-actin with 2.5 μM HPRF and 1.0 nM mDia1(FH2). Filament 1: control. Filament 2: mDia1(FH2) -associated.

concentration 3.3-fold for Bni1p and 4.7-fold for mDia1 (Figure 3A, closed squares and diamonds).

The rate of barbed-end elongation with each of the four FH1FH2 constructs has a biphasic dependence on the concentration of profilin (Figure 3B). An important technical point is that filament brightness allowed us to distinguish formin-associated and free barbed ends over a wide range of profilin concentrations (as described in Figures 2 and S3). In all cases, profilin increases elongation rate, with maximal effect in the range of 2–5 μM profilin, but inhibits elongation at higher concentrations. The amplitude of the increase in barbed-end elongation rate over that of free barbed ends varies from ~1.25-fold for Cdc12(FH1FH2)p to ~5-fold for mDia1 (FH1FH2) (Figure 3B, inverted closed triangles and open diamonds). For formin-associated filaments, the ratio of the barbed-end elongation rate with optimal profilin to the rate without profilin is infinitely higher for Cdc12p, 10-fold for mDia2, 5-fold for Bni1p, and 5-fold for mDia1.

On the other hand, the elongation rate of barbed ends associated with mDia1(FH2) (lacking the FH1 domain) decreases sharply from 0 to ~2.5 μM profilin and then plateaus (Figure 3D, diamonds). Thus, the FH1 domain is required for profilin to increase the elongation rate of barbed ends associated with an FH2 domain as well as for formin-dependent

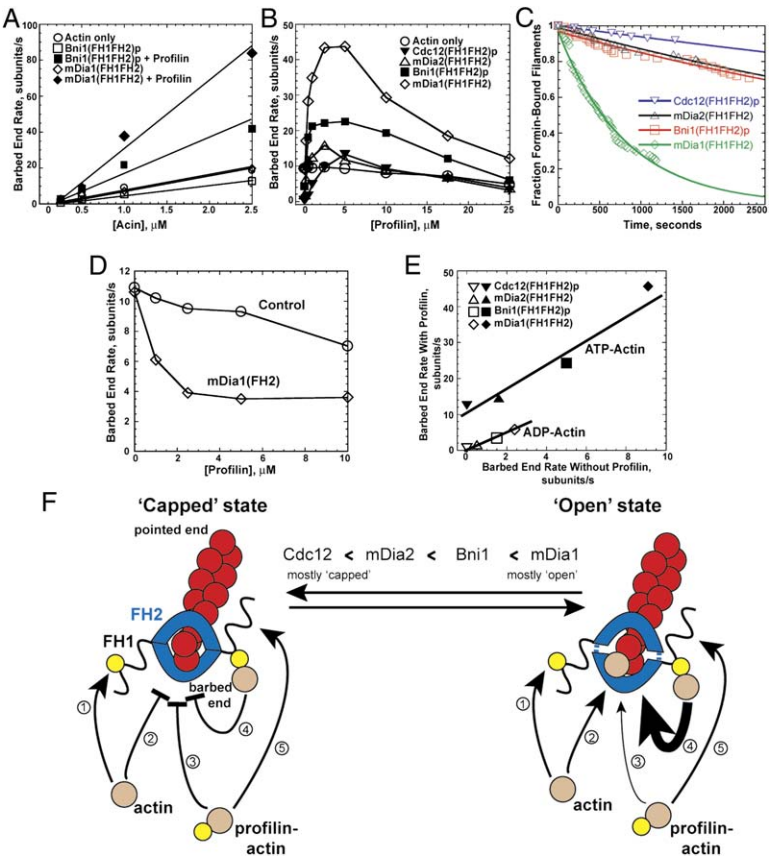

Figure 3. Effect of Actin and Profilin Concentration on Formin-Mediated Actin Elongation

(A) Dependence of the barbed-end elongation rate of formin-nucleated filaments on the concentration of ATP-actin in the absence or presence of 2.5 μM profilin (mDia1:HPRF, Bni1p:ScPRF).

(B) Dependence of the barbed-end elongation rate of formin(FH1FH2)p-associated filaments in the presence of 1.0 μM ATP-actin with 0.5 μM ATP-OG-actin on the concentration of profilin (Cdc12p: SpPRF; Bni1p: ScPRF; mDia1 and mDia2: HPRF).

(C) Dependence of the fraction of formin bound filaments on time, in the presence of 5.0 μM profilin. Exponential fits indicate dissociation rates of formin from the elongating barbed end: 1.2×10^{-3} s^{-1} for mDia1(FH1FH2); 1.3×10^{-4} s^{-1} for mDia2(FH1FH2); 1.3×10^{-4} s^{-1} for Bni1(FH1FH2)p; and 6.0×10^{-5} s^{-1} for Cdc12(FH1FH2)p.

(D) Dependence of the barbed-end elongation rate of 1.0 μM ATP-actin with 0.5 μM ATP-OG-actin (○) alone or in the presence of (◇) 1 nM mDia1(FH2) on the concentration of profilin (HPRF).

(E) Plot of the rate of barbed-end assembly without profilin (x axis) versus the barbed-end rate with profilin (y axis) for ATP-actin (filled symbols) and ADP-actin (open symbols) in the presence of various formins.

(F) Formin-mediated actin assembly model. Processive association of formin with the elongating barbed end is dependent upon the FH2 domain dimer, which encircles the end of the filament (Otomo et al., 2005). The FH2 dimer is in a rapid equilibrium between a "capped state" that does not allow addition of either actin or profilin-actin (left diagram: pathways 2, 3, and 4) and an "open state" (right diagram). The equilibrium constants ($K_{o/c}$) are: Cdc12p ~0.0, mDia2 ~0.3, Bni1p ~0.7, and mDia1 ~0.9. Actin monomers add directly to the barbed end when the FH2 domain is open (right pathway 2) or bind to profilin associated with an adjacent FH1 domain (pathway 1). Profilin-actin can add directly to an "open" end (right pathway 3), but at only a third the rate of actin, or to an adjacent FH1 domain (pathway 5) that contains from one to sixteen profilin binding sites depending upon the formin. Profilin-actin associated with the flexible FH1 domain assembles up to ~5-fold faster than actin alone (right pathway 4) because of favorable orientation for addition, an equilibrium shift toward the "open" FH2 domain state, and the local increase in actin concentration.

nucleation of profilin-actin (Kovar et al., 2003; Li and Higgs, 2003; Pring et al., 2003; Sagot et al., 2002b).

Effect of Mutant Profilins on Formin-Mediated ATP-Actin Assembly

Experiments with mutants confirmed that the effect of profilin on formin-mediated barbed-end elongation requires profilin binding to both actin and poly-L-proline (Kovar et al., 2003) and shows that profilin-actin can add directly to the barbed end of a formin-associated filament without interacting with the formin (Figure 3F, pathway 3) but at only a third the rate of free-actin monomers. We used human profilin point mutations with affinities for actin (profilin-R88E) or poly-L-proline (profilin-Y6D) reduced >100-fold (our unpublished data; Figure S4; Table 1).

The actin binding profilin mutant R88E does not change the elongation rate of barbed ends associated with either formin. mDia1-associated filaments grow at the same rate as control filaments alone or in the presence of profilin-R88E, and mDia2-associated filaments grow ~25% slower than control filaments alone or in the presence of profilin-R88E (Figures S4E and S4F and Figures S4M and S4N).

The poly-L-proline binding profilin mutant Y6D reduces the elongation rate of barbed ends associated with both formins by two-thirds. mDia1-associated filaments grow at 9.4 sub/s alone or at 3.2 sub/s in the presence of profilin-Y6D, and mDia2-associated filaments grow at 1.5 sub/s alone or at 0.5 sub/s in the presence of profilin-Y6D (Figures S4G and S4H and Figures S4O and S4P).

Formins Remain Processively Attached to Elongating Filament Barbed Ends in Both the Absence and Presence of Profilin

Unresolved questions concern the role of the FH1 domain and profilin in formin processivity. Results of others suggest that profilin binding to FH1 is required for FH2 processivity of mDia1(FH1FH2) (Romero et al., 2004), whereas we found that profilin is not needed for processive movement of

Bni1(FH1FH2)p (Kovar and Pollard, 2004). Since mDia1 (FH1FH2) does not alter the barbed-end elongation rate in the absence of profilin, experiments with soluble formin did not reveal if mDia1(FH1FH2)p is associated continuously with elongating barbed ends (Figure 1). Therefore, we attached mDia1 and mDia2 to slides also coated with NEM-myosin II to test their processivity. When NEM-myosin II captures filaments elongating with their barbed end attached to an immobilized formin, they are forced to buckle as they grow (Kovar and Pollard, 2004). Furthermore, the only way for a filament to buckle as it grows between immobilized formin and NEM-myosin II is for formin to be "on" the very end of the filament, not just "near" the end of the filament.

Two distinct populations of filaments grow from 1.0 μM actin monomers on slides coated with both NEM-myosin II and mDia2(FH1FH2) in the absence of profilin (Figures 4A–4C). Control filaments grow at their free barbed ends, which are not attached to the slide surface, at a rate of 7.3 subunits/s in this experiment (Filament 1). These filaments do not buckle. Filaments in the second population (Filament 2) buckle as they grow from their barbed ends attached to the slide surface at rates (~1.5 subunits/s) similar to barbed ends bound to mDia2(FH1FH2) free in solution (Filament 2 in Figures 1D–1F). Thus, mDia2(FH1FH2) moves processively with an elongating barbed end whether free in solution or immobilized on glass slides.

Similar to mDia2, two populations of filaments grow from 0.5 μM actin monomers in observation chambers coated with NEM-myosin II and GST-mDia1(FH1FH2) in the absence of profilin (Figures 4G–4I). Control filaments do not buckle as their free barbed ends grow at 6.0 subunits/s (Filament 1). Filaments in the second population buckle as they grow from their barbed end attached to the slide surface at 5.2 subunits/s (Filament 2). Thus, profilin is not required for processive movement of mDia1 or mDia2 on elongating barbed ends.

Addition of 2.5 μM profilin to these assays has no effect on the control filaments but increases elongation rates of buckling filaments associated with either mDia1 (~2-fold) or mDia2 (~5-fold) (Figures 4D–4F and 4J–4L) in a manner similar to that measured for these FH1FH2 constructs in solution (Figures 2 and 3A). The buckling filaments are half as bright as nonbuckling filaments in both cases.

Actin filament buckling is not due to traces of "active" myosin, since we have never observed buckling with only NEM-myosin on the slide (Figures 1 and 2, 5, S1 and S2, and S5; Amann and Pollard, 2001; Kovar et al., 2003; Kovar and Pollard, 2004; Kuhn and Pollard, 2005).

Formin-Mediated Assembly of ADP-Actin

ADP-OG-actin filaments are too dim for visualization, so we used actin labeled on lysine with Alexa green (AG-actin) for experiments on the assembly of Mg-ADP-actin monomers (Figures 5 and S5; Table 2). Unlike OG-actin labeled on cys-374, AG-actin labeled on lysine contributes fully to the rate of assembly in mixtures with unlabeled actin (R.M. and T.D.P., unpublished data). In the absence of formin, all filaments assembled from 3.0 μM ADP-actin are equally bright, as they elongate from their barbed ends at 3.9 subunits/s and their pointed ends at 0.05 subunits/s (Figures 5A–5C).

Two distinct populations of filaments assemble from ADP-actin in the presence of all FH1FH2 constructs except Cdc12p (Figures 5D–5L). Internal control filaments are equal in brightness and elongate at approximately the same rate as barbed ends in the absence of formin (Filament 1 in each case). Formin-associated filaments elongate significantly slower at their barbed ends than controls (Filament 2 in each case); the rate with mDia2 is ~7% of control filaments in the same sample (Figures 5D–5F); the rate with Bni1p is 22% of controls (Figure 5G–5I); and the rate with mDia1 is 31% of controls (Figure 5J–5L). In addition, formin-associated filaments are 25% dimmer than control filaments for all three FH1FH2 constructs, presumably because modification of lysine residues compromises addition of fluorescent actin onto ends associated with formin. Formin-associated dim filaments occasionally switch to growing at the faster control rate coincident with becoming bright, formin dissociation events (Filament 3 in each case). No Cdc12(FH1FH2)p-dependent filaments appear in samples with 3 μM Mg-ADP-actin, most likely because they remain too small to be detected during the 20 min time course.

Formin-Mediated Assembly of Profilin-ADP-Actin

To determine the affect of Cdc12(FH1FH2)p on the assembly of ADP-actin, as well as the affect of profilin on all four formins, we visualized the assembly of 5 μM ADP-actin. Profilin increases the barbed-end elongation rate of 5 μM ADP-actin in the presence of all four FH1FH2 constructs: from 0 to 0.7 subunits/s for Cdc12p, from 0.5 to 1.5 subunits/s for mDia2, from 1.6 to 2.4 subunits/s for Bni1p, and from 2.6 to 5.8 subunits/s for mDia1 (Figures 5M–5R and S5D–S5M; Table 2). Labeled lysine residues appear not to affect profilin binding, since profilin does not change the fluorescent intensity of elongating ADP-actin filaments in the presence of FH1FH2, which are still 25% dimmer than control filaments in the same sample. In the absence of formin all filaments are equally bright and grow at 7.3 subunits/s at their barbed ends and 0.18 subunits/s at their pointed ends (Figures S5A–S5C).

DISCUSSION

Our comparison of the activities of the formin-homology 1 and 2 domains (FH1FH2) from four formins (fission yeast Cdc12p, budding yeast Bni1p, mouse mDia1, and mouse mDia2) establishes that their mechanisms are similar (Figures 3A–3C, 3E, and 3F). However, the rates of the reactions vary so widely that assays less direct than observation of individual filaments can give misleading mechanistic impressions. All four formins nucleate actin filament assembly from ATP and ADP monomers. Cdc12p caps the barbed end while the other three allow elongation and remain continuously bound to the elongating barbed end in the presence of ATP-actin or ADP-actin. Profilin allows ATP- or ADP-actin to elongate barbed ends associated with Cdc12p and increases the elongation rate of barbed ends associated with the other three formins. The rates depend on the profilin concentration

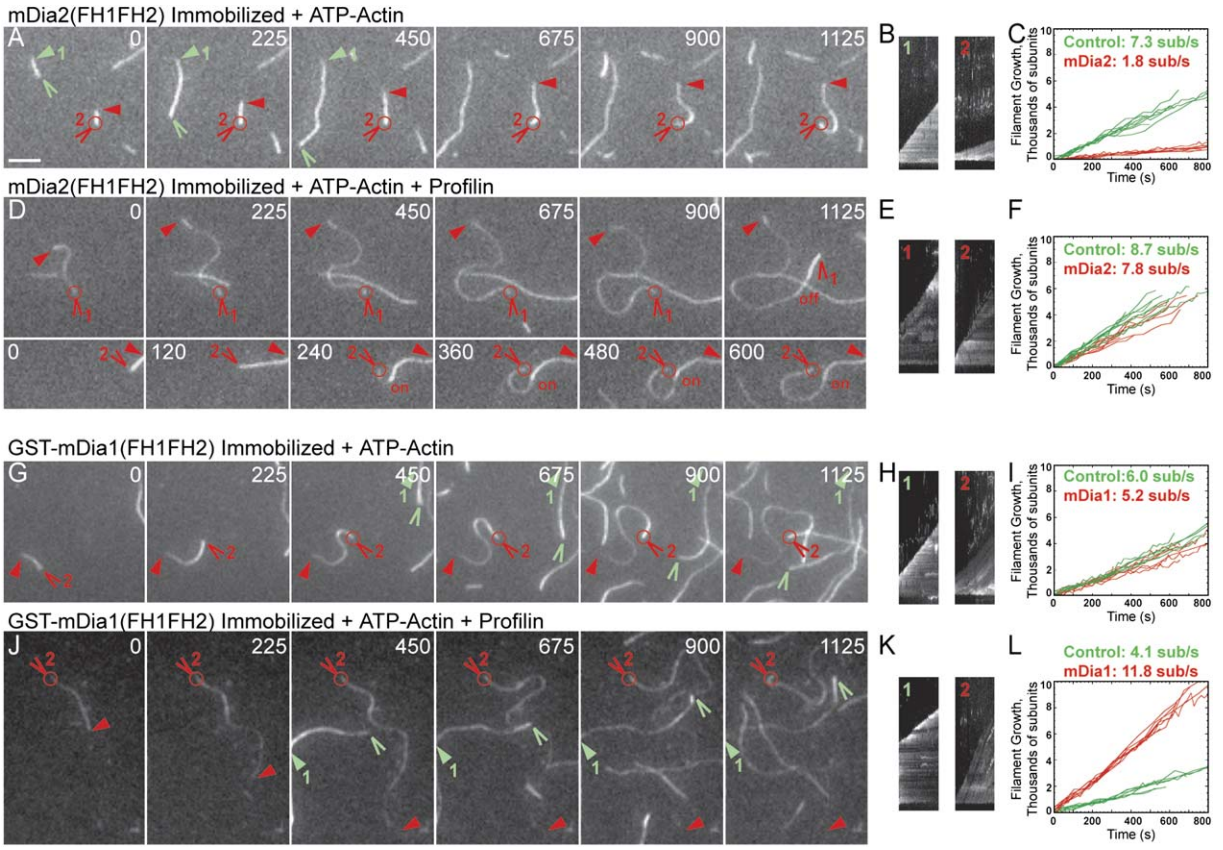

Figure 4. Time-Lapse Evanescent Wave Fluorescence Microscopy of Actin Filaments Growing from Formins Attached to the Slide Surface

Assembly of 1.0 μM ATP-actin with 0.5 μM OG-ATP-actin (A–F) or 0.5 μM ATP-actin with 0.25 μM OG-ATP-actin (G–L) on slides coated with formin and NEM-myosin II. Conditions and symbols as in Figure 1. Red circles indicate points where filaments were attached at their barbed end to formin or GST-formin on the slide surface. Scale bar = 5 μm.

(A, D, G, and J) Time-lapse micrographs with time in seconds indicated at the top. Green and red marks indicate control and formin-associated filaments.

(B, E, H, and K) Kymographs of the length (y axis) of the filaments marked to the left versus time (x axis, 900 s).

(C, F, I, and L) Plots of the growth of eight individual filament barbed ends versus time for control (both ends free) and formin-associated filaments.

(A–C) Assembly of 1.0 μM ATP-actin on a slide preincubated with mDia2(FH1FH2). Filament 1: control. Filament 2: mDia2(FH1FH2)-associated.

(D–F) Assembly of 1.0 μM ATP-actin with 2.5 μM HPRF on a slide preincubated with mDia2(FH1FH2). Filament 1: mDia2(FH1FH2) dissociates. Filament 2: mDia2(FH1FH2) associates.

(G–I) Assembly of 0.5 μM ATP-actin on a slide preincubated with GST-mDia1(FH1FH2). Filament 1: control. Filament 2: mDia1(FH1FH2)-associated.

(J–L) Assembly of 0.5 μM ATP-actin with 2.5 μM HPRF on a slide preincubated with GST-mDia1(FH1FH2). Filament 1: control. Filament 2: mDia1(FH1FH2)-associated.

in a biphasic fashion, up to 5-fold the diffusion-limited rate for ATP-actin addition onto barbed ends associated with mDia1 (Figure 3B).

Observation of individual filaments is required to appreciate the mechanism of formin-mediated actin assembly. Interpretation of the data from bulk assays depends on assumptions that are either difficult to verify (the concentration of elongating ends) or are false (assuming that the samples are homogeneous). Since formins both nucleate filaments and influence the rate of elongation at barbed ends, neither barbed-end concentrations nor elongation rates can be inferred by the rate of change of the polymer concentration in a bulk sample.

Direct observation of individual filaments reveals the heterogeneity of filaments in the presence of formins and allows measurements on different species in the population. In fact the heterogeneity is a virtue, because some filaments in each sample have free barbed ends and serve as internal controls for comparison with formin-associated filaments in the same field. In some cases, the two populations can be distinguished simply by their elongation rates, but under other circumstances the fluorescence intensity of the filaments elongating in association with a formin is lower than filaments with free barbed ends. In both cases, sudden changes in elongation rate (and fluorescence intensity) reveal formin association or dissociation events.

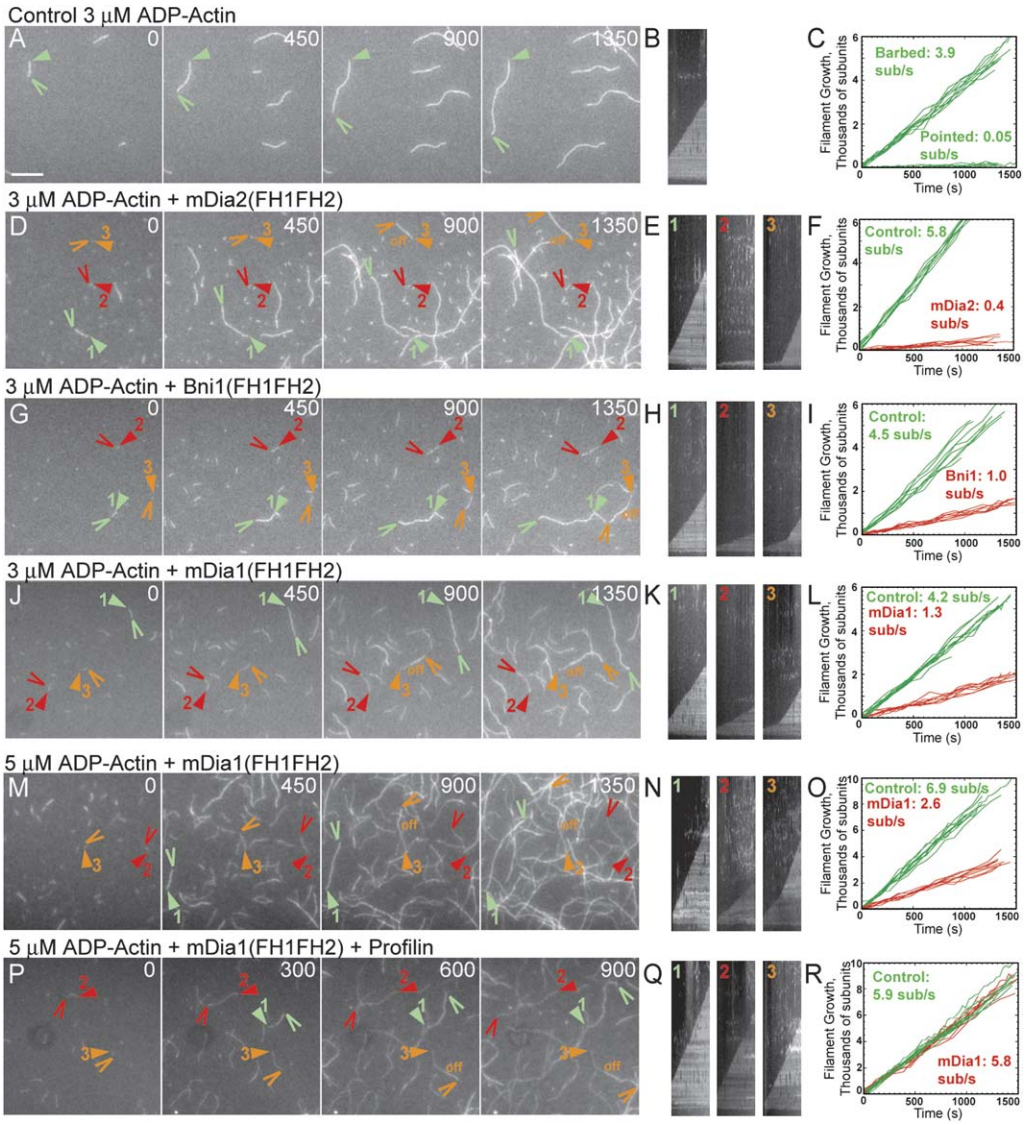

Figure 5. Time-Lapse Evanescent Wave Fluorescence Microscopy of the Effect of Formins on ADP-Actin Polymerization

The spontaneous assembly of 2.25 μM ADP-actin with 0.75 μM ADP-actin labeled with Alexa green (ADP-AG-actin; [A–L]) or 3.75 μM ADP-actin with 1.25 μM ADP-AG-Actin (M–R) on slides coated with NEM-myosin II. Conditions: 10 mM imidazole (pH 7.0), 50 mM KCl, 1 mM $MgCl_2$, 1 mM EGTA, 50 mM DTT, 0.2 mM ADP, 50 μM $CaCl_2$, 15 mM glucose, 20 μg/ml catalase, 100 μg/ml glucose oxidase, 0.5% (4000 cP) methylcellulose, 0.1 units hexokinase, at 25ºC. Symbols as in Figure 1. Scale bar = 5 μm.

(A, D, G, J, M, and P) Time-lapse micrographs with time in seconds indicated at top. Green, red, and orange marks indicate control, formin-nucleated, and filaments where formin dissociates (off) during the time course.

(B, E, H, K, N, and Q) Kymographs of the length (y axis) of the filaments marked to the left versus time (x axis, 900 s).

(C, F, I, L, O, and R) Plots of the growth of eight individual filament barbed ends (and pointed ends for [C]) versus time for control and formin-nucleated filaments.

(A–C) 3 μM ADP-actin only control.

(D–F) 3 μM ADP-actin with 1.0 nM mDia2(FH1FH2). Filament 1: control. Filament 2: mDia2(FH1FH2)-nucleated. Filament 3: mDia2(FH1FH2) dissociates.

(G–I) 3 μM ADP-actin with 5.0 nM Bni1(FH1FH2)p. Filament 1: control. Filament 2: Bni1(FH1FH2)p-nucleated. Filament 3: Bni1(FH1FH2)p dissociates.

(J–L) 3 μM ADP-actin with 1.0 nM mDia1(FH1FH2). Filament 1: control. Filament 2: mDia1(FH1FH2)-nucleated. Filament 3: mDia1(FH1FH2) dissociates.

(M–O) 5 μM ADP-actin with 1.0 nM mDia1(FH1FH2). Filament 1: control. Filament 2: mDia1(FH1FH2)-nucleated. Filament 3: mDia1(FH1FH2) dissociates.

(P–R) 5 μM ADP-actin with 6.0 μM profilin (HPRF) and 1 nM mDia1(FH1FH2). Filament 1: control. Filament 2: mDia1(FH1FH2)-associated. Filament 3: mDia1(FH1FH2) dissociates.

Table 2. Comparison of ADP-Actin Assembly Rates in the Presence of Formin

Conditions[b]	Elongation Rate (Control Filaments[a])	
	Barbed-End Subunits/s	Pointed-End Subunits/s
3 μM ADP-Actin[c]		
3 μM ADP-actin only	3.9 ± 0.08	0.05 ± 0.01
mDia2(FH1FH2)	0.4 ± 0.02 (5.8 ± 0.04)	0.02 ± 0.02 (0.1 ± 0.05)
Bni1(FH1FH2)p	1.0 ± 0.02 (4.5 ± 0.08)	0.07 ± 0.01 (0.08 ± 0.03)
mDia1(FH1FH2)	1.3 ± 0.02 (4.2 ± 0.03)	0.10 ± 0.03 (0.1 ± 0.02)
5 μM ADP-Actin[d]		
5 μM ADP-actin only	7.3 ± 0.2	0.18 ± 0.1
5 μM ADP-actin + 6 μM profilin	6.2 ± 0.09	0.01 ± 0.008
Cdc12(FH1FH2)p	NA[e] (8.7 ± 0.06)	0.27 ± 0.02 (0.26 ± 0.05)
Cdc12(FH1FH2)p + 6 μM profilin	0.70 ± 0.02 (5.3 ± 0.06)	0.08 ± 0.01 (0.05 ± 0.04)
mDia2(FH1FH2)	0.5 ± 0.04 (9.7 ± 0.1)	0.17 ± 0.01 (0.31 ± 0.03)
mDia2(FH1FH2) + 6 μM profilin	1.5 ± 0.05 (6.1 ± 0.07)	0.01 ± 0.02 (0.04 ± 0.04)
Bni1(FH1FH2)p	1.6 ± 0.05 (6.4 ± 0.1)	0.21 ± 0.08 (0.18 ± 0.03)
Bni1(FH1FH2)p + 6 μM profilin	2.4 ± 0.06 (6.1 ± 0.09)	0.03 ± 0.01 (0.04 ± 0.02)
mDia1(FH1FH2)	2.6 ± 0.05 (6.9 ± 0.1)	0.11 ± 0.03 (0.15 ± 0.05)
mDia1(FH1FH2) + 6 μM profilin	5.8 ± 0.06 (5.9 ± 0.04)	0.02 ± 0.02 (-0.05 ± 0.03)

[a] The rates of internal control filaments are reported in parentheses.
[b] At least ten individual filaments were measured for each population. Rates are represented as mean ± SD. Formin was not attached to the slide surface, as reported in Figures 5 and S5.
[c] 2.25 μM unlabeled ADP-actin and 0.75 μM ADP-AG-actin.
[d] 3.75 μM unlabeled ADP-actin and 1.25 μM ADP-AG-actin.
[e] Cdc12-nucleated filaments elongate from their pointed ends only.

Mechanism for Actin Filament Elongation in Association with Formins

Our new observations provide enough information to frame a general mechanism for formin-mediated processive actin assembly (Figure 3F). The mechanism involves equilibrium between two formin conformations on the end of the filament and five additional reactions of profilin, actin, and actin-profilin with the formin and the end of the filament. The process is complex, but most of the rate and equilibrium constants are known, so it has been possible to formulate a mathematical model of these reactions that accounts for most of the data in this paper (Vavylonis et al., 2006). Here, we focus on the experimental challenges and controversies. Characterization of additional formin isoforms is required to determine whether all formins are mechanistically similar with the four evolutionarily diverse formins studied here.

Each of the four formins tested has a characteristic effect on the rate of barbed end elongation rate, but no effect on pointed-end elongation. Compared with the elongation of free barbed ends in the same samples (100%), the elongation rates are zero for Cdc12p, 25% for mDia2, 50%–75% for Bni1p, and 90% for mDia1. These reductions in elongation rate are the same over a range of ATP-actin concentrations (Figure 3A), so they are intrinsic properties of the formins.

We agree with the proposal of Otomo et al. (2005) that formins have at least two conformations or states when bound to barbed ends—a capped state that precludes addition of a subunit to the end and an open state that allows subunit addition. Our interpretation of the range of effects of formins on barbed-end elongation rates is that each has a different equilibrium constant for the partition between the open/capped states of the formin FH2 domains. The open/capped equilibrium is far on the side of capped for Cdc12p ($K_{o/c}$ ~0), far on the side of open for mDia1 ($K_{o/c}$ ~0.9), and intermediate for the other two formins. These equilibria are rapid because filaments elongate at rates proportional to the actin concentration up to 80 subunits/s (Figure 3A). Other parameters, such as different rates of actin addition and/or subtraction from the barbed end in the open state, may also contribute to differences in elongation rates in the presence of the various formin FH2 domains.

The basis for this intrinsic difference between FH2 domains is not known, but the equilibrium between capped and open may be influenced by the linker length between the two subunits in the formin dimer (Xu et al., 2004). The Cdc12p linker is short, whereas the mDia1 linker is longer, and the mDia2 and Bni1p linkers are intermediate.

Profilin Increases the Rate of Formin-Mediated Barbed-End Elongation

Bulk assays led to uncertainty about the effect of profilin on formin-mediated actin assembly. In a few cases, profilin slightly increased the rate of formin-mediated polymerization (Kovar et al., 2003; Moseley et al., 2004; Sagot et al., 2002b), but in most cases profilin decreased the polymerization rate (Harris et al., 2004; Kobielak et al., 2004; Li and Higgs, 2003; Pring et al., 2003; Romero et al., 2004). This disparity results from two opposing effects of profilin, which inhibits nucleation but increases the rate of FH1FH2-mediated barbed-end elongation (Kovar et al., 2003).

Profilin increases the rate of elongation of barbed ends associated with formin FH1FH2 domains, providing that the profilin can interact with both actin and polyproline. The rate depends on the particular formin and the concentration of profilin. Formin-associated filaments are readily distinguished in experiments with OG-actin because their fluorescence intensity is less than control filaments. At optimal profilin concentrations, barbed-end elongation rates for all four formins are higher than control filaments, up to ~5-fold higher than controls for mDia1. Romero et al. (2004) reported that profilin and mDia1 increased the barbed-end elongation rate 15-fold over free barbed ends. Their mDia1(FH1FH2) construct contained 11 putative profilin binding sites. Our mDia1(FH1FH2) construct contains only five putative profilin binding sites (Li and Higgs, 2003), but the maximum elongation rate for a construct with 11 profilin binding sites is also ~5-fold greater than control filaments (Table 1). It is possible that Romero overestimated the maximum rate of elongation by including only the longest 20% of filaments in their analysis.

With all four formins, the elongation rate increases up to a maximum within 2.5 to 5 μM profilin and then declines at higher profilin concentrations (Figure 3B). Optimal profilin concentrations saturate the actin monomer pool. High concentrations of free profilin reduce the elongation rate by competing with profilin-actin for binding FH1 (see Vavylonis et al. [2006] for a quantitative explanation). We note that profilin enhances elongation of ends associated with FH1FH2 in spite of the fact that actin bound to profilin actually adds to ends associated with FH2 at one third the rate of free actin monomers (Figures 2J–2L). Accordingly, profilin that binds actin but not polyproline slows down elongation of barbed ends associated with FH1FH2 barbed ends.

The effect of profilin on the four formins is inversely proportional to their barbed-end elongation rate without profilin. The effect of profilin is greatest on Cdc12p, since profilin increases the rate of barbed-end elongation from 0 to over 10 subunits/s (Figure 3B). Profilin increases the barbed-end elongation rate of mDia2 10-fold from 1.5 to 15 subunits/s, of Bni1p 5-fold from 5 to 25 subunits/s, and of mDia1 5-fold from 9 to 45 subunits/s. Three mechanisms may contribute to the ability of profilin to increase the rate of barbed-end elongation:

(1) Tethering profilin-actin to an FH1 adjacent to the end of the filament might increase the probability that actin collides with the barbed end in an orientation favorable for binding. Only ~2% of freely diffusing actin monomers are oriented favorably for binding to barbed ends during a collision (Drenckhahn and Pollard, 1986), so a small change in the orientation factor from 0.02 to about 0.10 could account for the enhancement of elongation.

(2) Profilin-actin binding to the FH1 domain may influence the open/capped equilibrium of FH2. This is most impressive in the case of Cdc12p(FH1FH2) where the presence of profilin overcomes capping. We note that profilin alone does not shift the equilibrium toward open, because profilin mutants that bind polyproline but not actin do not increase the elongation rate (Kovar et al., 2003; Figure S4; Table 1).

(3) Raising the local concentration of profilin-actin several orders of magnitude by association with multiple polyproline motifs in FH1 might overcome capping without a shift in the open/capped equilibrium. However, this requires that $K_{o/c}$ for Cdc12(FH1FH2)p be greater than 0, and we have not yet detected elongation of barbed ends associated with Cdc12(FH1FH2)p without profilin. We note that the absolute rate of elongation is roughly proportional to the number of potential profilin binding sites in the FH1 domains of the four formins. FH1 domains from Cdc12p and mDia2 have only two putative profilin binding sites, while the FH1 domains from Bni1p and mDia1 contain three and five (to eleven). However, since the fold increase in elongation rate with profilin is inversely related to the number of profilin binding sites (profilin increases Cdc12p and mDia2 the most), and since mDia1 constructs containing five and eleven profilin binding sites elongate at the same rate, the barbed-end elongation rate is not simply proportional to the number of profilin binding sites.

Processive Attachment of Formins to Growing Barbed Ends in the Absence and Presence of Profilin

Our observations of individual actin filaments elongating in the presence of formins free in solution or immobilized on microscope slides show that all four formins remain continually attached to the barbed end in both the absence and presence of profilin. Cdc12p in the absence of profilin simply caps barbed ends (Kovar et al., 2003; Kovar and Pollard, 2004), and the other three formins remain attached while allowing insertional assembly of new subunits. Thus, the processive elongation mechanism originally proposed (Pruyne et al., 2002) and supported by bulk assays (Harris et al., 2004; Moseley et al., 2004; Zigmond et al., 2003) for Bni1p is applicable to diverse formins from widely divergent species.

Romero et al. (2004) proposed that formins require profilin for processivity and suggested that, in the absence of profilin, mDia1(FH2) and mDia1(FH1FH2) are in rapid equilibrium with, but do not stay continually bound to, the growing barbed end. They argued that rapid barbed-end equilibria explain the ability of formins to allow barbed-end elongation in

the presence of excess capping protein in the absence of profilin (Harris et al., 2004; Moseley et al., 2004; Zigmond et al., 2003). Romero et al. (2004) proposed that profilin makes mDia1(FH1FH2) processive by binding to the FH1 domain, interacting with the ultimate and penultimate actin subunits and then walking along the end of the actin filament like a child swinging on ''monkey bars.''

Our direct observations show unambiguously that barbed ends associated with the mouse formins mDia1 and mDia2 elongate processively with ATP-actin both with and without profilin. Furthermore, mDia1 FH2 (Figures 2J–2L) and Bni1 FH2 (Table 1) alone are sufficient for processive attachment at elongating barbed ends. We do not observe filaments growing at rates intermediate between the rate of control actin and the reduced rate supported by formin alone or the accelerated rate supported by formin with profilin. Formins occasionally dissociate from an occupied end, or bind to a free end, whereupon both the rate of elongation and the intensity of the fluorescence switch simultaneously to the rates characteristic of a free or an occupied end. The existence of these two filament populations in the same sample strongly suggests that formins remain continually attached to elongating filament barbed ends. Processive association was verified by visualization of filaments growing from formin immobilized on slides (Figure 4; Table 1). Since formins dissociate from elongating barbed ends extremely slowly in both the absence and presence of profilin (1×10^{-4} s^{-1} for Bni1p; Kovar and Pollard, 2004; Figure 3C), the ''run length'' of formin on the barbed end of an elongating actin filament is impressively long (at least 40,000 to 200,000 subunits on average depending upon the formin).

The mechanism that allows formin FH2 domains to maintain processive association with an elongating barbed end is not entirely understood (Figure 3F). As predicted from the lack of rotation of filaments elongating from an immobilized formin (Kovar and Pollard, 2004), the Bni1 FH2 domain dimer wraps around a dimer of rhodamine-labeled actin in a co-crystal like a shaft in a bearing (Otomo et al., 2005). Flexibility between the two halves must allow the FH2 dimer to move onto new subunits as they add to the end of a filament. Most proposals (Harris et al., 2004; Moseley et al., 2004, Otomo et al., 2005; Romero et al., 2004; Xu et al., 2004; Zigmond et al., 2003) involve each of the two formin subunits tracking along one of the long pitch actin helices. Unless formins immobilized on slides spin relative to the slide, our microscopic observations of buckling filaments are more consistent with a mechanism whereby the FH2 dimer rotates around the filament axis as each new subunit is added. Alternatively, it has been theorized that the FH2 domain dimer could relax torsion stresses by rotating in specific steps in the direction opposite to the rotation direction of the long pitch actin helices (Shemesh et al., 2005).

ATP-Hydrolysis Is Not Required for Processive Elongation of Barbed Ends Associated with Forming

Romero et al. (2004) proposed that ATP-hydrolysis provides energy for formin processivity because profilin increased the rate of ATP-hydrolysis during mDia1-mediated assembly of Ca-ATP-actin and because they did not observe actin with bound AMP-PNP to elongate filaments associated with mDia1. We find that formins nucleate filaments from ADP-actin and remain continually associated with barbed ends elongating by addition of Mg-ADP-actin. This demonstrates that ATP hydrolysis is not required for processive elongation by formins in the presence or absence of profilin. These reactions with ADP-actin are slow for two reasons. First, ADP-actin is much less active than ATP-actin. Second, Bni1p, mDia1 and mDia2 all slow elongation by ADP-actin more than ATP-actin. This is evidence that the conformation of FH2 domains on barbed ends is sensitive to the nucleotide bound to actin, with $K_{o/c}$ being lower for ADP-actin than ATP-actin.

Thus, rather than favoring barbed-end elongation (Romero et al., 2004), ATP hydrolysis and dissociation of γ-phosphate actually make elongation less favorable. We agree with Romero et al. (2004) that the free energy change associated with actin subunit binding to the end of the filament is the likely alternative to ATP-hydrolysis as the free energy source to move the formin on the end of the filament. Investigating whether or not formins influence the hydrolysis of ATP when filaments elongate in the presence of Mg-ATP-actin will require quench-flow methods originally used to show that profilin does not increase the rate of ATP hydrolysis during actin elongation (Blanchoin and Pollard, 2002).

EXPERIMENTAL PROCEDURES

Plasmid Constructs and Protein Purification

Bacterial expression constructs, protein purification, and preparation of ATP- and ADP-actin are described in Supplemental Experimental Procedures.

TIRF Microscopy

Time-lapse evanescent wave fluorescence microscopy was performed and analyzed as described (Amann and Pollard, 2001; Kovar et al., 2003; Kovar and Pollard, 2004; Kuhn and Pollard, 2005). Images from an Olympus IX-70 inverted scope were collected every 15 s with a Hamamatsu C4742-95 CCD camera (Orca-ER) and processed with ImageJ software (http://rsb.info.nih.gov/ij/).

Glass flow cells (5 × 25 × 0.3 mm; lwh) were incubated with either 10 nM *N*-ethyl maleimide (NEM) myosin or NEM-myosin and 100 nM mDia2(FH1FH2) or 100 nM GST-mDia1(FH1FH2) for 1 min, washed extensively with 1% BSA, equilibrated with TIRF buffer (10 mM imidazole [pH 7.0], 50 mM KCl, 1 mM $MgCl_2$, 1 mM EGTA, 50 mM DTT, 0.2 mM ATP, 50 μM $CaCl_2$, 15 mM glucose, 20 μg/ml catalase, 100 μg/ml glucose oxidase, 0.5% [4000 cP] methylcellulose), and mounted on the microscope for imaging. Mixtures of either unlabeled Ca-ATP actin and Ca-ATP OG-actin, converted to Mg-ATP actin by adding 0.2 volume of 1 mM EGTA and 0.25 mM $MgCl_2$ for 5 min at 25ºC or unlabeled ADP-actin and ADP Alexa green (AG)-actin, were mixed with 2× TIRF buffer supplemented with water and formin or profilin to give the final concentrations indicated in the figure legends. Samples were then transferred to a flow cell for imaging.

We analyzed TIRF experiments by measuring the lengths of 20–25 randomly chosen filaments (throughout the entire field) every three to four frames for at least 48 frames. Plots of length versus time for barbed and pointed ends of individual filaments (Figure S1E) identified distinct filament populations and gave the average rate (subunits/s) of each population. To display TIRF experiments, we selected from the 135 × 110 μm recorded field of view a representative 35 × 35 μm area (Figure S1A) containing examples of all filament populations and displayed this area as a montage of three to six frames to illustrate the time series (Figure S1B). The movies are

published as Supplemental Data. We then selected and marked representative filaments from each population within the 35 × 35 μm region and traced their lengths for 60 frames (900 s) to create kymographs (Figure S1C) that show the change in filament length (y axis) over time (x axis).

Supplemental Data

Supplemental Data include five figures, twenty movies, and Supplemental Experimental Procedures and can be found with this article online at http://www.cell.com/cgi/content/full/124/2/423/DC1/.

ACKNOWLEDGMENTS

This work was supported by NIH Grants GM-2613 and GM-26338 (to T.D.P.) and GM-069818 (to H.N.H.), a Pew Biomedical Scholars award (to H.N.H), an NIH Postdoctoral Fellowship (to D.R.K.), and an NIH Training Grant T32 GM08704 (to E.S.H.).

Received: June 28, 2005
Revised: August 24, 2005
Accepted: November 10, 2005
Published: January 26, 2006

REFERENCES

Amann, K.J., and Pollard, T.D. (2001). Direct real-time observation of actin filament branching mediated by Arp2/3 complex using total internal reflection fluorescence microscopy. Proc. Natl. Acad. Sci. USA *98*, 15009–15013.

Blanchoin, L., and Pollard, T.D. (2002). Hydrolysis of ATP by polymerized actin depends on the bound divalent cation but not profilin. Biochemistry *41*, 597–602.

Chang, F., Drubin, D., and Nurse, P. (1997). cdc12p, a protein required for cytokinesis in fission yeast, is a component of the cell division ring and interacts with profilin. J. Cell Biol. *137*, 169–182.

Drenckhahn, D., and Pollard, T.D. (1986). Elongation of actin filaments is a diffusion-limited reaction at the barbed end and is accelerated by inert macromolecules. J. Biol. Chem. *261*, 12754–12758.

Evangelista, M., Pruyne, D., Amberg, D.C., Boone, C., and Bretscher, A. (2002). Formins direct Arp2/3-independent actin filament assembly to polarize cell growth in yeast. Nat. Cell Biol. *4*, 260–269.

Feierbach, B., and Chang, F. (2001). Roles of the fission yeast formin for3p in cell polarity, actin cable formation, and symmetric cell division. Curr. Biol. *11*, 1656–1665.

Harris, E.S., Li, F., and Higgs, H.N. (2004). The mouse formin, FRLalpha, slows actin filament barbed end elongation, competes with capping protein, accelerates polymerization from monomers, and severs filaments. J. Biol. Chem. *279*, 20076–20087.

Higashida, C., Miyoshi, T., Fujita, A., Oceguera-Yanez, F., Monypenny, J., Andou, Y., Narumiya, S., and Watanabe, N. (2004). Actin polymerization-driven molecular movement of mDia1 in living cells. Science *303*, 2007–2010.

Higgs, H.N., and Peterson, K.J. (2005). Phylogenetic analysis of the formin homology 2 domain. Mol. Biol. Cell *16*, 1–13.

Kobielak, A., Pasolli, H.A., and Fuchs, E. (2004). Mammalian formin-1 participates in adherens junctions and polymerization of linear actin cables. Nat. Cell Biol. *6*, 21–30.

Kovar, D.R., and Pollard, T.D. (2004). Insertional assembly of actin filament barbed ends in association with formins produces piconewton forces. Proc. Natl. Acad. Sci. USA *101*, 14725–14730.

Kovar, D.R., Kuhn, J.R., Tichy, A.L., and Pollard, T.D. (2003). The fission yeast cytokinesis formin Cdc12p is a barbed end actin filament capping protein gated by profilin. J. Cell Biol. *161*, 875–887.

Kovar, D.R., Wu, J.Q., and Pollard, T.D. (2005). Profilin-mediated competition between capping protein and formin Cdc12p during cytokinesis in fission yeast. Mol. Biol. Cell *16*, 2313–2324.

Kuhn, J.R., and Pollard, T.D. (2005). Real-time measurements of actin filament polymerization by total internal reflection fluorescence microscopy. Biophys. J. *88*, 1387–1402.

Li, F., and Higgs, H.N. (2003). The mouse Formin mDia1 is a potent actin nucleation factor regulated by autoinhibition. Curr. Biol. *13*, 1335–1340.

Moseley, J.B., Sagot, I., Manning, A.L., Xu, Y., Eck, M.J., Pellman, D., and Goode, B.L. (2004). A conserved mechanism for Bni1- and mDia1-induced actin assembly and dual regulation of Bni1 by Bud6 and profilin. Mol. Biol. Cell *15*, 896–907.

Otomo, T., Tomchick, D.R., Otomo, C., Panchal, S.C., Machius, M., and Rosen, M.K. (2005). Structural basis of actin filament nucleation and processive capping by a formin homology 2 domain. Nature *433*, 488–494.

Pellegrin, S., and Mellor, H. (2005). The Rho family GTPase Rif induces filopodia through mDia2. Curr. Biol. *15*, 129–133.

Petersen, J., Nielsen, O., Egel, R., and Hagan, I.M. (1998). FH3, a domain found in formins, targets the fission yeast formin Fus1 to the projection tip during conjugation. J. Cell Biol. *141*, 1217–1228.

Pring, M., Evangelista, M., Boone, C., Yang, C., and Zigmond, S.H. (2003). Mechanism of formin-induced nucleation of actin filaments. Biochemistry *42*, 486–496.

Pruyne, D., Evangelista, M., Yang, C., Bi, E., Zigmond, S., Bretscher, A., and Boone, C. (2002). Role of formins in actin assembly: nucleation and barbed-end association. Science *297*, 612–615.

Romero, S., Le Clainche, C., Didry, D., Egile, C., Pantaloni, D., and Carlier, M.F. (2004). Formin is a processive motor that requires profilin to accelerate actin assembly and associated ATP hydrolysis. Cell *119*, 419–429.

Sagot, I., Klee, S.K., and Pellman, D. (2002a). Yeast formins regulate cell polarity by controlling the assembly of actin cables. Nat. Cell Biol. *4*, 42–50.

Sagot, I., Rodal, A.A., Moseley, J., Goode, B.L., and Pellman, D. (2002b). An actin nucleation mechanism mediated by Bni1 and profilin. Nat. Cell Biol. *4*, 626–631.

Shemesh, T., Otomo, T., Rosen, M.K., Bershadsky, A.D., and Kozlov, M.M. (2005). A novel mechanism of actin filament processive capping by formin: solution of the rotation paradox. J. Cell Biol. *170*, 889–893.

Schirenbeck, A., Bretschneider, T., Arasada, R., Schleicher, M., and Faix, J. (2005). The Diaphanous-related formin dDia2 is required for the formation and maintenance of filopodia. Nat. Cell Biol. *7*, 619–625.

Schutt, C.E., Myslik, J.C., Rozycki, M.D., Goonesekere, N.C., and Lindberg, U. (1993). The structure of crystalline profilin-beta-actin. Nature *365*, 810–816.

Severson, A.F., Baillie, D.L., and Bowerman, B. (2002). A formin homology protein and a profilin are required for cytokinesis and Arp2/3-independent assembly of cortical microfilaments in *C. elegans*. Curr. Biol. *12*, 2066–2075.

Vavylonis, D., Kovar, D.R., O'Shaughnessy, B., and Pollard, T.D. (2006). Model of formin-associated actin filament elongation. Mol. Cell, in press.

Vinson, V.K., De La Cruz, E.M., Higgs, H.N., and Pollard, T.D. (1998). Interactions of Acanthamoeba profilin with actin and nucleotides bound to actin. Biochemistry *37*, 10871–10880.

Xu, Y., Moseley, J.B., Sagot, I., Poy, F., Pellman, D., Goode, B.L., and Eck, M.J. (2004). Crystal structures of a formin homology-2 domain reveal a tethered dimer architecture. Cell *116*, 711–723.

Zigmond, S.H., Evangelista, M., Boone, C., Yang, C., Dar, A.C., Sicheri, F., Forkey, J., and Pring, M. (2003). Formin leaky cap allows elongation in the presence of tight capping proteins. Curr. Biol. *13*, 1820–1823.